International Journal of Natural Resources and Environmental Studies
ISSN: 3006-2012 (Print), ISSN: 3006-0834 (Online) | Volume 2, Number 2, Year 2024
DOI: https://doi.org/10.62051/ijnres.v2n2.18
Journal homepage: https://wepub.org/index.php/IJNRES/index

Numerical Simulation of Proppant Transportation and Placement Law In Fractured Coal Reservoirs

Xingyue Chu

College of Energy Science and Engineering, Henan University of Science and Technology, Jiaozuo 454000, Henan, China

ABSTRACT

Hydraulic fracturing technology has been widely used in the development of low-permeability oil fields, gas fields, and coalbed methane. The morphology of the sand dike formed by proppant deposition in the fracture determines the effective shape of the fracture, the effective volume, the flow conductivity, and the validity period of the fracture, and the research on the proppant transport law in the fracture is of great significance in optimizing the fracturing construction parameters and improving the fracturing production increase effect. In this paper, a systematic study on the proppant transport law in hydraulic fracturing fracture is carried out by numerical simulation, which reveals the mechanism of proppant settling and transport, clarifies the proppant transport and placement law under different working conditions, and puts forward the optimization strategy of hydraulic fracturing process on the basis of this study.

KEYWORDS

Hydraulic fracturing; Proppant; Transport law; Fluent numerical simulation; Fracturing process optimization.

1. INTRODUCTORY

At present, it is an urgent challenge to substantially increase the output of a single well of coalbed methane (CBM). Coalbed methane reservoir is a dual-structured pore system composed of pores and fractures, which is characterized by a low-permeability porous medium[1]. The small pore size and large number of coal matrix pores are the main contributors to the pore specific surface area, which provides sufficient space for CBM storage[2]. The fracture system of CBM reservoirs is the main channel for fluid penetration in coal. Hydraulic fracturing utilizes a high-pressure pumping unit on the surface to pump fracturing fluid into the bottom of the well at a displacement that far exceeds the suction capacity of the formation, and then hold the pressure at the bottom of the well to generate high pressure, which causes fractures when the pressure exceeds the ground stress and tensile strength of the rock[3-6], and then pumps sand-carrying fluid with proppant in accordance with a certain sand ratio, which expands the formed hydraulic fracture forward and effectively supports it, and then, when the fracturing construction is finished, the fracture is closed on the proppant, forming a fracture with a proppant in the formation, and then a fracture with the proppant in the formation. After the fracturing, the fracture closes on the proppant, forming sand-filled fractures with high inflow capacity in the formation, thus realizing the increase of production and injection of oil and gas wells[7-10]. The settlement and transportation of proppant has an important influence on the activation of natural single fractures and the formation of complex fracture channels to a certain extent, and the formation of artificial fractures through effective proppant placement is an important criterion for measuring the effectiveness of fracturing construction[11-14], and the sand placement pattern of proppant in the fracture has a direct influence on the flow-conducting capacity of proppant fractures[15,16]. Therefore, it is very necessary to study the settlement and transportation law of proppant within single and complex cracks.

Based on the above, this paper adopts the research method of numerical simulation to study the transportation law of proppant in single and complex cracks. Fluent numerical simulation software is used to study the placement of proppant under different reservoir pressures, to establish a model for solving the change of fracture inflow capacity caused by different conditions, and to further understand the factors affecting the placement of proppant and fracture inflow capacity, so as to provide theoretical guidance for the optimization of hydraulic fracturing scheme and field construction.

2. SIMULATION METHODOLOGY AND MODELING

2.1. Mathematical model

Multiphase flow is a flow and heat exchange process in which one fluid and another (or more) immiscible fluid or solid mix with each other in a certain flow region. In this paper, a proppant transport model is developed to simulate the process of fracturing fluid carrying proppant transporting and settling in the fracture. The Eulerian model is used to track the movement state and settlement distribution law of the proppant in the solid-liquid two-phase flow process[17].

Based on the theory of fluid mechanics, the law of conservation of mass and energy must be obeyed during the movement of fluid[18-20].

(1) mass conservation equation

$$\frac{\partial}{\partial_t}(\alpha_l \rho_l) + \nabla (\alpha_l \rho_l \overrightarrow{v_l}) = 0 \tag{1-1}$$

$$\frac{\partial}{\partial_t}(\alpha_s \rho_s) + \nabla (\alpha_s \rho_s \overrightarrow{v_s}) = 0 \tag{1-2}$$

where α is the volume fraction, m/s; ρ is the density, kg/m^3; v is the velocity, m/s; t is the time, s; and in the subscript l is the liquid phase and s is the solid phase.

(2)conservation of momentum equation

$$\frac{\partial}{\partial_t}(\alpha_l \rho_l \overrightarrow{v_l}) + \nabla \cdot (\alpha_l \rho_l \overrightarrow{v_l}\overrightarrow{v_l}) = -\alpha_l \nabla p + \nabla \cdot \tau_l + \alpha_l \rho_l g + \beta(\overrightarrow{v_s} - \overrightarrow{v_l}) \tag{1-3}$$

$$\frac{\partial}{\partial_t}(\alpha_s \rho_s \overrightarrow{v_s}) + \nabla \cdot (\alpha_s \rho_s \overrightarrow{v_s}\overrightarrow{v_s}) = -\alpha_s \nabla p + \nabla \cdot \tau_s + \alpha_s \rho_s g + \beta(\overrightarrow{v_l} - \overrightarrow{v_s}) \tag{1-4}$$

Where: p is the partial pressure, Pa; ꞇ is the shear stress tensor, Pa; g is the gravitational acceleration taken as 9.8 m/s^2; β is the interphase momentum exchange coefficient, $kg/(m^3 \cdot s)$.

2.2. Model building

(1) geometric model

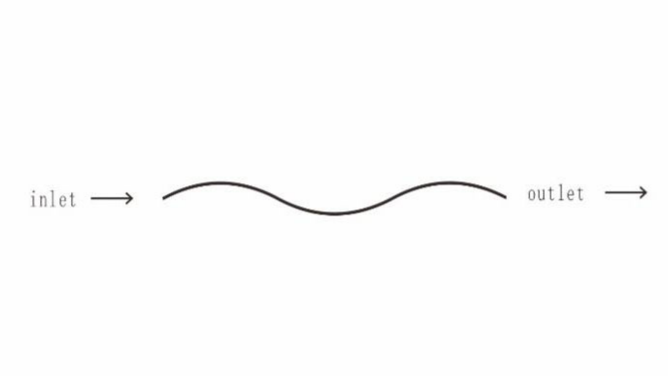

A single crack

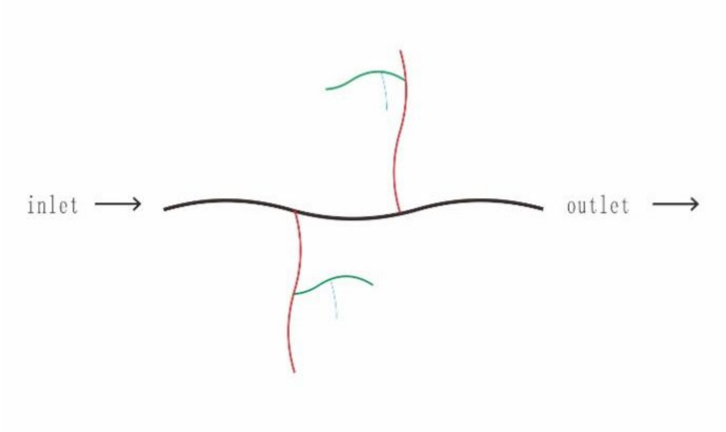

B Complex cracks

Figure 1. Design of 2 types of morphological cracks

The numerical model is based on common complex intersecting cracks and simulates cracks with different morphologies, including single cracks and complex cracks. The single crack size is 1200 mm × 5 mm × 2 mm (Fig. 1A); the complex crack has a primary crack size of 1200 mm × 5 mm × 2 mm (black), a secondary crack of 600 mm × 40 mm × 1.5 mm (red), a tertiary crack of 400 mm × 30 mm × 1.2 mm (green), and a tertiary crack of 200 mm × 20 mm × 0.8 mm (blue) (Fig. 1B). The left side of the crack is the inlet of sand-carrying fluid, and the right side is the outlet.

(2) Grid division

The geometric model is divided using hexahedral structured mesh using the pre-processing software Mesh, and the crack mesh division is shown in Figure 2. The number of grid nodes for single crack division is 255883, and the number of cells is 1121731; the number of grid nodes for complex crack division is 532418, and the number of cells is 2199685.

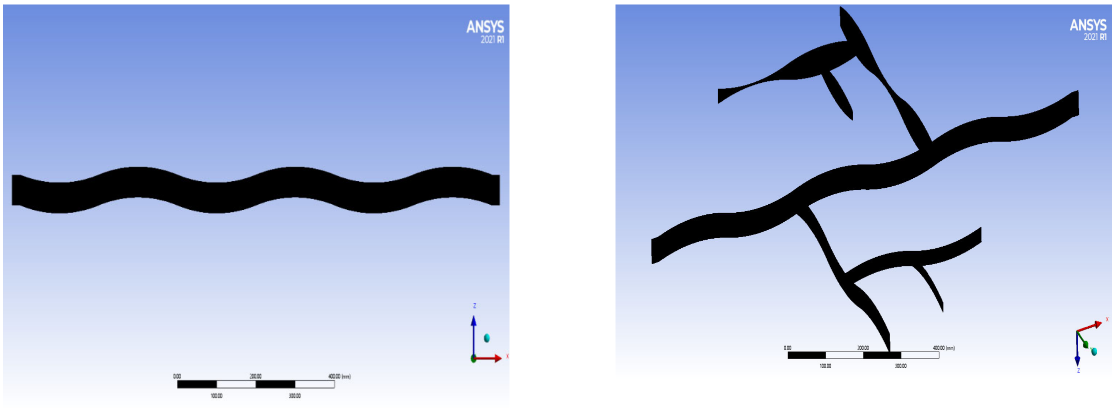

Schematic mesh delineation of single crack   Schematic mesh delineation of complex cracks

Figure 2. Schematic diagram of crack mesh delineation

2.3. Simulation area and parameter setting

To establish the model of proppant transport in the crack, the Eulerian multiphase flow model is chosen to simulate the particle flow by treating the proppant as a proposed fluid. It is assumed that the wall surface is smooth, the temperature is constant and the wall pressure is variable. The k-ε turbulence model is used to describe the flow of the proppant inside the fracture, and the fracture interior is set to be filled with fracturing fluid, and the Simple algorithm is used to solve the pressure and velocity coupling field, with the pressure in the standard discrete format, and all others in the first-order discrete format. The setup simulation parameters are shown in Table 1.

Table 1. Engineering parameter setting table

Displacement /(m·s-1)	Fracturing fluid viscosity /(mPa·s)	Sand ratio /%	Wall pressure /(MPa)	Proppant density/(kg·m-3)
6	1	6	5	
8	2	8	10	2600
10	3	10	15	

3. RESULTS AND ANALYSIS

3.1. Crack morphology

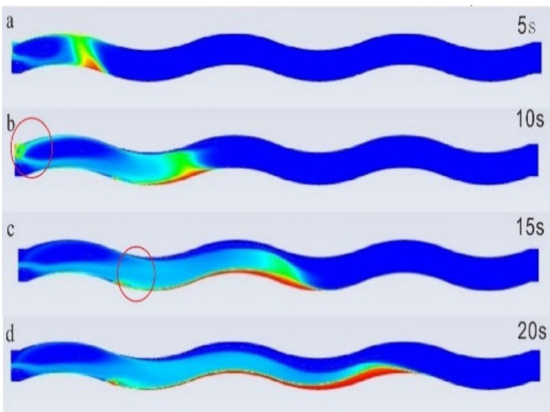

Figure 3. Single crack proppant volume fraction distribution

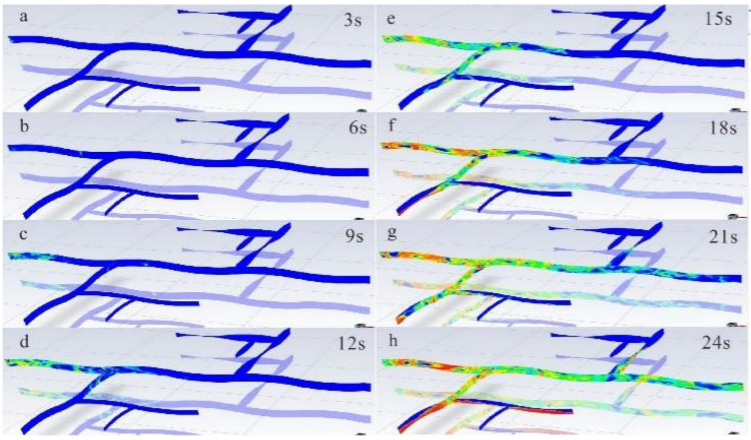

Figure 4. Complex crack proppant volume fraction distribution

In order to study the influence of different fracture morphology on proppant transportation, the viscosity of fracturing fluid was set at 1 mPa-s, the displacement at 10 m/s, the density of proppant at 2660 kg/m^3, and the sand ratio at 8%, and the experiments of proppant in a single fracture and a complex fracture were carried out respectively. Comparing the distribution characteristics of proppant in different cracks, it is found that the crack morphology has a significant effect on the proppant transportation law.

Among them, the distribution of proppant within a single crack is uniform, and the distribution of proppant volume fraction in a single crack is shown in Fig. 3. According to the observation of the simulation process, the turbulence effect near the crack entrance at the pumping time of 10s causes multiple vortices, which suspends the particles in the crack, and eventually forms a sand-free zone at the front end of the crack. At 15s the proppant accumulation increases, the proppant is subject to the blocking effect of the wall at the turn, the channel narrows, the collision with the wall increases, etc. and causes stall settlement, which leads to the formation of a proppant aggregation region. As the height of the sand dike increases, the proppant is transported forward by the buoyancy of the sand-carrying liquid in the vertical direction and the drag force in the horizontal direction, and the height of the sand pile stops growing, i.e., it reaches the equilibrium height, when the amount of deposition at the top of the sand dike is balanced with the volume carried by the sand-carrying liquid erosion.

The formation process of sand dike inside the crack in complex cracks is the same as in single cracks, as shown in Fig. 4. When the pumping time is 12s, the proppant will be carried into the branch cracks under the liquid carrying effect, but the quantity is small. With the deposition of proppant in the main crack, the height of the sand bank increases, and after reaching the equilibrium height, the proppant starts to enter the branch crack under the effect of fluid carryover, particle rolling, and suspension state transport. At 18s, the proppant can be seen passing through the branch cracks, which is hindered by the steering of the crack channel, resulting in the reduction of the flow rate of the sand-carrying fluid and its impact on the crack wall in the process of transportation and stalled settlement, and then the sand dike is formed. When the time is 24s, the proppant in the branch crack reaches the equilibrium height and starts to transport to the secondary branch. This is due to the fact that the proppant slides along the surface of the sand dike to fill the deeper part of the branch cracks, thus increasing the effective length of the branch cracks, which leads to the fact that the branch cracks that are closer to the entrance of the main crack are filled better than the branch cracks that are located farther away from the entrance of the main crack.

Combined with the above analysis, it is believed that it is relatively easy to place the proppant in the first-stage branch fractures connected to the main fractures, while it is more difficult to enter the second-stage and higher-stage fractures for filling, and when the branch fractures are filled to a certain extent, the flow resistance will prompt the proppant to extend in the main fractures mainly, which indicates that the multi-stage branch fractures greatly increase the flow resistance of the proppant in the fractures, and the fracturing process of complex fractures should be adopted as much as possible when fracturing at the site. Large displacement should be used as much as possible.

3.2. Sand ratio

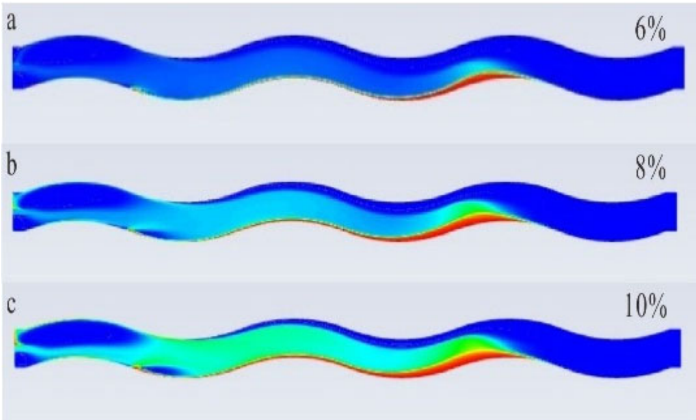

Figure 5. Proppant volume fraction distribution under different sand ratios in single fracture

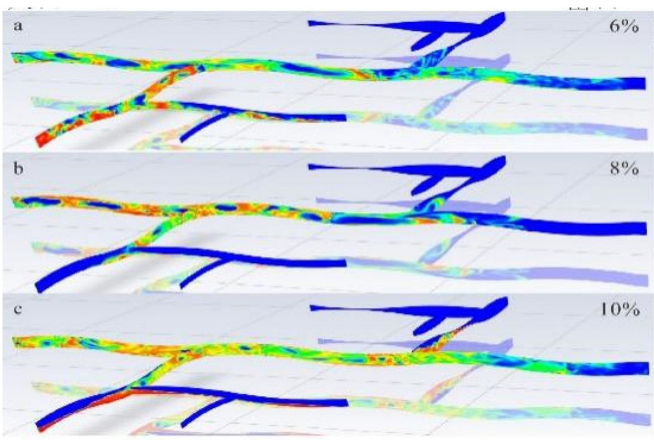

Figure 6. Proppant volume fraction distribution under different sand ratios in complex fracture

In order to study the effect of sand ratio on proppant transportation, the viscosity of fracturing fluid was set at 1 mPa-s, the displacement was 8 m/s, the density of proppant was 2660 kg/m3, and the sand ratios were set at 6%, 8%, and 10%, respectively. Comparing the distribution characteristics of proppant in the cracks under different sand ratios, it was found that the proppant laying patterns in the cracks corresponding to different sand ratios were relatively similar.

From Fig. 5, it can be seen that under the same displacement, the morphology of the sand bank formed by the three sand ratios is basically the same, and the difference in equilibrium height is not significant. When the fracturing fluid carries the proppant into the fracture, under the action of gravity, the proppant particles gradually settle and accumulate, forming a sand dike. With the increase of sand ratio, the number of proppant particles per unit volume increases, which is equivalent to increasing the viscosity of sand-carrying fluid. The mutual interference between particles becomes stronger, resulting in a decrease in the horizontal transportation speed of particles and a decrease in the settling speed, which ultimately leads directly to a decrease in the flow rate of single particles, a decrease in the settling speed, and a decrease in the settling volume. On the other hand, due to the increase of sand concentration in the sand-carrying liquid, the amount of proppant deposition increases.

Therefore, the proppant deposition patterns in the cracks corresponding to different sand ratios are relatively similar. Comparatively speaking, the equilibrium height of the sand dike is higher when the sand ratio is set to 10%, which is more conducive to improving the fracture inflow capacity.

As shown in Fig. 6 under the same conditions, the main crack and the single crack in the complex crack are similar, and the proppant placement patterns corresponding to different sand ratios have little effect. When the sand ratio is set to 10%, the amount of proppant entering the branch crack, the laying area and the distance increase significantly, which is due to the narrower width of the branch crack wall, the increase in the number of proppant entering the crack per unit time, increasing the viscosity of the sand-carrying liquid, increasing the collision between the proppant particles as well as the particles and the wall, and the frictional resistance increases so that the more the proppant settles down. From the simulation results, it can be seen that due to the increase in the volume fraction of proppant, the proppant interaction in the branch fracture is enhanced, and more proppant particles enter the branch fracture. However, in order to prevent fracture blockage caused by too high sand ratio during early pumping, it is recommended to increase the sand ratio appropriately to improve the proppant efficiency during construction.

3.3. Fracturing fluid viscosity

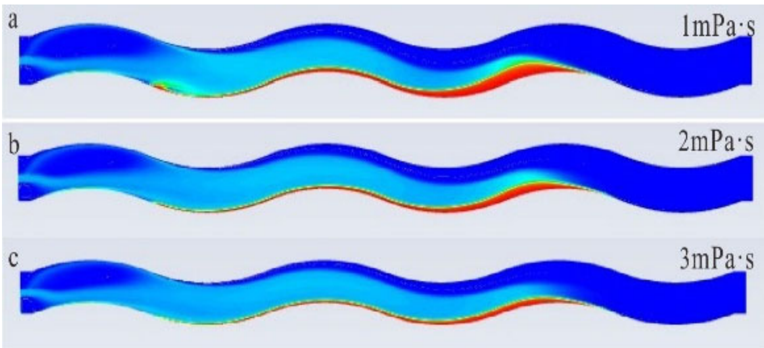

Figure 7. Proppant volume fraction distribution under different viscosity conditions in single fracture

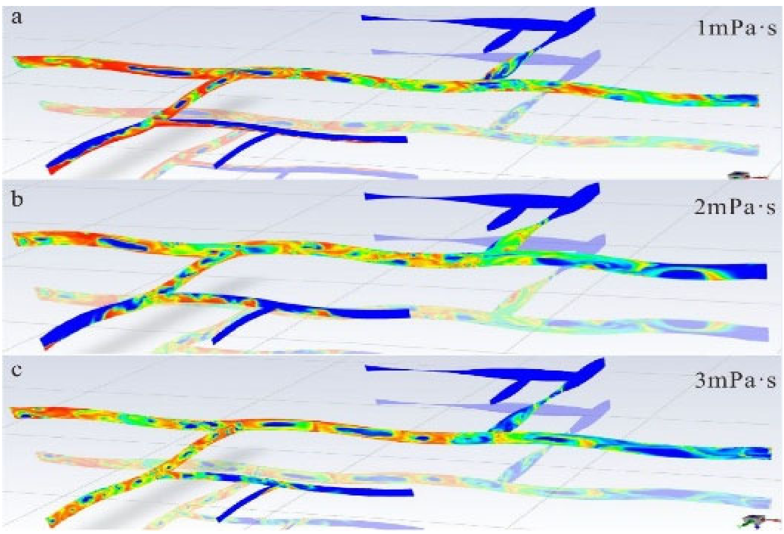

Figure 8. Proppant volume fraction distribution under different viscosity conditions in complex fracture

In order to study the effect of fracturing fluid viscosity on proppant transport, the displacement of fracturing fluid was set at 8m/s, sand ratio at 8%, proppant density at 2660kg/m3, and the solution with viscosity of 1mPa-s was used to simulate the active water fracturing fluid, 2mPa-s was used to simulate the three-anti-fracturing fluid, and 3mPa-s was used to simulate the three-anti and one-drop fracturing fluid.

According to Stokes' formula in Fig. 7, when active water fracturing fluid is used, the proppant is deposited at the entrance under the influence of gravity, and the proppant transportation distance increases with the increase of the discharge volume, showing a trend of gradual decrease in the amount of deposition from the entrance to the exit, and the slope of the stacking shape becomes more and more gentle and the distribution is more uniform. With the increase of viscosity, the sand-carrying capacity increases and the sedimentation rate decreases. The proppant can be transported to the farther end of the fracture with the fracturing fluid when the three-proof and one-down fracturing fluid is used, indicating that the proppant transport ability is enhanced.

In complex fractures, it can be seen from Fig. 8 that with the increase of fracturing fluid viscosity, the height of proppant in the main fracture and branch fracture decreases obviously, and the proppant enters the tertiary fracture to form a certain volume of sand dike, and the main fracture and the secondary fracture are well laid. The equilibrium time of the pumping process is shortened, the proppant is more transported to the depth of the fracture, and the support range of the complex fracture is increased and distributed more evenly. It can be seen that the nature of fracturing fluid has a certain degree of influence on the proppant transport distance and placement pattern, so the use of three anti-fracturing fluids can effectively increase the sand-carrying capacity of fracturing fluid to enhance the proppant transport distance, the proppant placement area is larger, the support range is wider, the filling of the main fracture and the branch fracture is improved, which is conducive to the effective placement of the proppant in the fracture.

3.4. Wall pressure

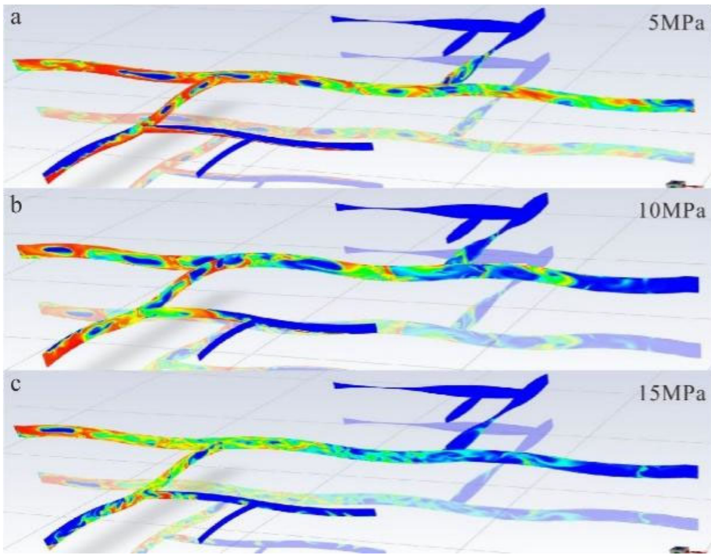

Figure 9. Proppant volume fraction distribution under different wall pressure conditions in complex cracks

In order to study the effect of wall pressure on proppant transportation, the viscosity of fracturing fluid was set to be 1 mPa-s, the displacement was 8 m/s, the sand ratio was 8%, the density of proppant was 2660 kg/m3, and the wall pressures were set to be 5 MPa, 10 MPa, and 15 MPa, respectively.

The proppant volume fraction distribution under different wall pressure conditions in the complex fracture is shown in Fig. 9. The flow-conducting ability of the fractured crack decreases with the increase of the closure pressure, because the closure pressure will make the proppant embedded in the wall of the crack, resulting in the increase of the particle gap, the width of the closure crack decreases slowly with the increase of the closure pressure, the flow-conducting ability of the crack decreases, and it is difficult for the proppant to settle and accumulate inside the crack. The more the proppant settles and spreads within the main crack, the larger the gap between particles. The crack wall will affect the force on the proppant particles, which will have an interfering effect on the proppant settlement and transportation, so that the proppant will mainly settle at the entrance of the crack, and it will be difficult to be transported to the distal end of the crack, which will lead to a reduction in the distance of proppant transportation, and a reduction in the equilibrium height. In branch cracks, due to the diversion effect, the proppant transportation speed is reduced, and the energy of sand-carrying liquid is reduced, which is also easy to cause the proppant to settle. As the wall pressure increases, the flow resistance inside the crack increases, and the fluid pressure drop gradually increases, which drives the wall deformation of the proppant-filled area inside the crack to increase, and affects the overall inflow capacity of the crack. When the wall pressure is 15MPa, the proppant is not easy to enter the branch fracture, the equilibrium height is reduced, and the proppant accumulation at the fracture turning place is obviously reduced. Corresponding to the actual fracturing in the field, with the increase of closure pressure, the degree of proppant embedding is gradually obvious, and the influence on the fracture flow-conducting ability is intensified, which affects the fracturing effect of coalbed methane wells.

4. CONCLUDE

In this paper, a numerical simulation study on the proppant transport and placement law was carried out by using FLUENT numerical simulation software, and the simulation analysis was carried out through four influencing factors, namely, fracture morphology, sand ratio, viscosity of sand-carrying liquid, and wall pressure, to reveal the transport and placement law of the proppant under different influencing factors. The main conclusions are as follows:

(1) The simulation of different fracture patterns reveals that the proppant transportation and placement laws in the main fracture of the complex fracture are highly similar to those in the single fracture. Compared with the single main fracture, the branch fracture within the complex fracture has a diverting effect, and when the branch fracture is filled to a certain degree, the flow resistance will prompt the proppant to extend mainly within the main fracture, and the multistage branch fracture greatly increases the flow resistance of the proppant within the fracture. When hydraulic fracturing is carried out on site, the hydraulic fracturing process of complex fractures should be carried out with large displacement as much as possible.

(2) The simulation of different sand ratios shows that the main fracture within the complex fracture is similar to a single fracture, and the proppant placement pattern corresponding to different sand ratios has little effect. When the sand ratio is large, the settlement in the branch cracks at all levels is relatively large, which is favorable to the proppant placement efficiency. However, in order to prevent the problem of fracture blockage caused by too high sand ratio during early pumping, it is recommended to increase the sand ratio appropriately to improve the fracture support effect during the hydraulic fracturing construction process.

(3) Simulation of different viscosities of sand-carrying fluids shows that the increase of viscosity of sand-carrying fluids is conducive to the increase of proppant transportation capacity, which is helpful for the long-distance transportation of proppant. With the functions of "waterproof sensitivity, quick sensitivity prevention, waterproof locking and low friction resistance", the three-proof and one-lower fracturing fluid is a low-harm fracturing fluid with excellent performance, which is able to realize the purpose of increasing CBM production and at the same time, effectively increase the sand-carrying capacity of the sand-carrying fluid, enhance the distance of proppant transportation, so that the proppant can be spread over a larger area with a wider range of support, and improve the effectiveness of propping in the main fracture and branch joints. The filling of the main and branch seams of the fracture is conducive to the effective laying of the proppant in the fracture.

(4) The simulation of different wall pressures found that the inflow capacity of fractured cracks decreases with the increase of closure pressure. As the closure pressure increases, the proppant is not easy to enter into the branch cracks, the equilibrium height decreases, and the proppant buildup at the crack steering is obviously reduced, which leads to the decrease of the fracture flow-conducting capacity. In the actual construction, the concentration of sand spread inside the fractured crack should be increased as much as possible to reduce the broken embedded proppant caused by the closure pressure, so as to realize the high flow-conducting capacity inside the crack.

ACKNOWLEDGMENTS

Paper Funding: Science and Technology Tackling Project of Henan Province (232102321139)

Natural Science Foundation of Henan Province (242300420222)

Project of "Double First-class" Discipline Creation Project of Safety and Energy Engineering Department of Henan University of Science and Technology (AQ20230715)

Special Funds for Basic Research Operating Expenses of Universities in Henan Province (NSFRF240811)

BIBLIOGRAPHY

[1] Gidley J L. Recent advances in hydraulic fracturing[J]. Richardson, TX (USA); Society of Petroleum Engineers, 1989.

[2] ZHONG Zhuo, LIU Zhanli, WANG Tao, et al. Key mechanical issues of hydraulic fracturing in shale[J]. Science Bulletin, 2016, 61(1): 72-81.

[3] JIANG Ruizhong, JIANG Tingxue, WANG Yongli. Recent development and prospect of hydraulic fracturing technology[J]. Oil Drilling Technology, 2004, 26(4): 52-57.

[4] Gao Q. Study on proppant inflow capacity and distribution law in staggered fracture network[D]. Northeast Petroleum University, 2024.

[5] Zhang Yang. Current status and development of horizontal well fracturing technology[J]. Shandong Chemical Industry, 2022, 51(02): 73~75.

[6] Cao Enming. Analysis of key technologies for hydraulic fracturing of oil reservoirs[J]. Chemical Engineering and Equipment, 2023(09): 99-100+95.

[7] ZHU Jian, HU Guo-Zhong, XU Jia-Lin, et al. Influence of coal seam stratigraphy on the effect of microwave breakthrough[J/OL]. Journal of Coal: 1-15[2024-04-11].

[8] Liu H. Characteristics of pore structure of No.3 coal in Hudi well field[J]. Coal, 2022, 31(10): 18-24.

[9] Zhang Q. Principles and Design of Oil Recovery Engineering[M]. China University of Petroleum Press, 2006.

[10] Yang W, Lu C, Si G, et al. Coal and gas outburst control using uniform hydraulic fracturing by destress blasting and water-driven gas release[J]. Journal of Natural Gas Science and Engineering, 2020, 79.

[11] Lu W, Huang B, Zhao X. A review of recent research and development of the effect of hydraulic fracturing on gas adsorption and desorption in coal seams[J]. Adsorption Science Technology, 2019, 37(5-6): 509-529.

[12] Fan Z, Yang T. Mechanical analysis and numerical simulation of a forming fracture network in the roof of an outburst coal seam by multi-staged fracturing[J]. Arabian Journal of Geosciences, 2022, 15(4): 289~310.

[13] Lu G, Xiangtao K, Gun H, et al. Experimental Study on Crack Extension Rules of Hydraulic Fracturing Based on Simulated Coal Seam Roof and Floor[J]. Geofluids, 2022, 45(20): 67~89.

[14] Xiao S, Ge Z, Cheng L, et al. Gas migration mechanism and enrichment law under hydraulic fracturing in soft coal seams: a case study in Songzao coalfield[J]. Energy Sources Part A Recovery Utilization and Environmental Effects, 2019: 1-15.

[15] ZHAO Hongbing. Factors affecting the production capacity of horizontal well volume fracturing in tight oil reservoirs and prediction methods[J]. Liaoning Chemical Industry, 2021, 50(01): 96-99.

[16] Tian Y, Tian Y, Qu Z, et al. A new experimental simulation method for the development of non-renewable hydrogen energy—Oil and gas resources[J]. International Journal of Hydrogen Energy, 2018, 44(11).

[17] Fjaestad D, Tomac I. Experimental investigation of sand proppant particles flow and transport regimes through narrow slots[J]. Elsevier, 2019.

[18] J. L. Gidley, Gidley, Gidley, et al. New developments in hydraulic fracturing technology [M]. Petroleum Industry Press, 1995.

[19] Li L, Wu W. Directional hydraulic fracturing technology for prefabricated longitudinal guide seams in a coal mine tight sandstone roof: [J]. Energy Exploration & Exploitation, 2022, 40(1): 400-420.

[20] Shaojie Z, Liang Z, Kai D. Experimental study on gas adsorption and drainage of gas-bearing coal subjected to tree-type hydraulic fracturing[J]. Energy Reports, 2022, 8649-660.